Organic-Inorganic Hybrid Coatings for High-Performance Protective Coatings Applications

Vijay Mannari *, H.R. Asemani, L. Lou

Coating Research Institute (CRI), Eastern Michigan University, 430 West Forest Ave. Ypsilanti, Michigan, 48197 USA

***** Corresponding author

E-mail: vmannari@emich.edu

Phone Number: (734) 487 1235

Fax: (734) 487 8755

Abstract

Organic-inorganic hybrid (OIH) thin films and coatings derived by the aqueous sol-gel process have emerged as promising alternatives to toxic and hazardous anti-corrosion pretreatments in multi-coat metal finishing operations. However, there are a number of technical and operational challenges associated with their application and performance. A sustainable photo-initiated sol-gel process has been developed to deposit OIH films on metal surfaces that efficiently address these challenges while providing corrosion protection comparable to conventional sol-gel systems. Wet films of non-aqueous compositions containing specially designed organo-silane precursors and photo-latent catalysts –photo-acid generator (PAG) or photo-base generators (PBG)-, produced cured OIH films by the sol-gel reaction when exposed to specific UV radiation under ambient moisture environment. In the present study, the corrosion performance of OIH films based on two families of organo-silane precursors cured by PAG and PBG have been compared with those obtained by the conventional sol-gel process. The effects of functionality, type of photocatalyst, UV intensity, cure conditions, and film thickness on corrosion resistance performance of OIH coatings have been studied using various qualitative and quantitative techniques such as DC polarization, electrochemical impedance spectroscopy (EIS), and accelerated salt spray test. Results revealed that by using proper precursor structure, photo-latent catalyst and under appropriate processing conditions, OIH pre-treated samples (7-8 μm) showed corrosion current density as low as 1.2 nA/cm^2 which is superior compared to conventional Cr (VI) pretreatments. The study clearly demonstrates the feasibility and benefits of this sustainable photo-initiated sol-gel process for many advanced applications.

Keywords: Sol-gel, UV curing, Corrosion resistance, Photo-latent catalyst, Organic-inorganic hybrid

1. Introduction

The metal finishing industry uses multilayer coating systems for long-term protection and aesthetics of the finished goods. In a typical system, the bare clean metal surface is first coated with a pretreatment layer, followed by a primer coat, a topcoat and optionally a protective clear coat. The pretreatment layer is very critical and important as it is expected to provide good adhesion to a metal surface and to the subsequent organic layer, as well as to provide corrosion resistance on the finished surface. For Al and Al-alloys, the use of Cr(VI) based conversion pretreatments provides excellent performance and hence they had been the undisputed choice of pretreatments [1], [2]. However, due to the toxic and carcinogenic profile of Cr(VI), its use is heavily regulated and industries across the globe are looking for effective alternatives to chromium-based systems [3], [4]. There have been different approaches in order to develop environmentally friendly pretreatments with comparable performance to that of Cr(IV) pretreatments [5], [6]. During the past decade, organic-inorganic hybrid (OIH) thin films and coatings based on Si compound derived by the sol-gel process have emerged as promising alternatives to toxic and hazardous anti-corrosion pretreatments [7], [8]. Their hybrid structure (organic and inorganic parts) enables them to provide a unique balance of barrier properties, mechanical performance, and desirable compatibility with topcoats. Moreover, superior adhesion could be achieved due to their ability for covalent bonding with a substrate and with the subsequently applied layers [9].

In a typical sol-gel process, as shown in **Figure 1**, silane groups are hydrolyzed in the presence of acid or base catalyst to form silanol groups (sol formation). Silanol groups formed then generate siloxane linkages (gel formation) either by self-condensation or by reaction with other silane groups. If starting material is a multi-functional organo-silane precursor, cross-linked organo-siloxane (organic-inorganic) network structure is formed. By the suitable choice of sol-gel precursor, its chemical structure and functionality, catalyst type, amount of water, and cure

conditions, the morphology of organic-inorganic network, and hence the coating properties can be effectively controlled [10].

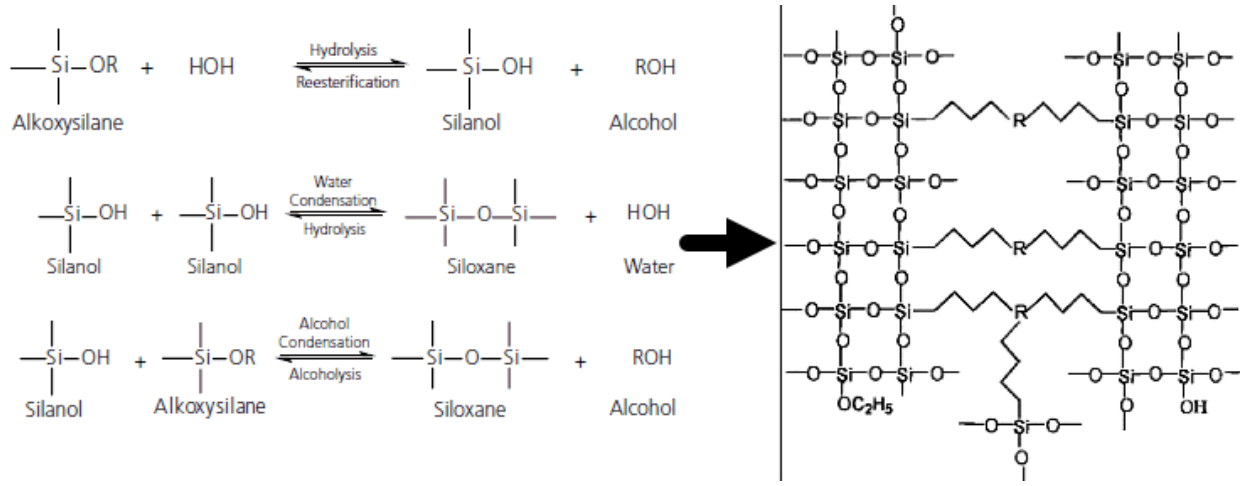

Figure 1: The mechanism of hydrolysis and condensation in the sol-gel process leading to silica thermoset network

There have been numerous studies in order to improve the performance of the sol-gel OIH pretreatments by varying the structure of silane precursors (e.g. chemistry, and functionality), incorporation of additives such as corrosion inhibitors, metal oxides, and nano-particles [11]–[18]. Our research group has recently come up with a series of OIH pretreatments that could perform comparably to chromate conversion coatings under appropriate application conditions [19]–[21]. Despite many advantages, these OIH pretreatments are associated with some limitations. The conventional sol-gel process is typically done by dipping metal parts into an acidic or basic dispersion of precursor in water/alcohol mixture (wet process). Continuous sol to gel conversion in the application bath will result in instability of the application bath and generation of a large amount of liquid waste after every refill. Bath stability is known to decrease by increasing the precursor's concentration [20]. Therefore, there is a limitation in bath concentration and film thickness (up to 10 µm). The sensitivity of the wet sol-gel process to pH variations also limits the substrate options for these pretreatments [22].

Among various efforts in order to enhance the time and cost efficiency of sol-gel systems, curing of sol-gel coatings using ultraviolet (UV) radiation is one promising solution [22]–[26]. In the presence of a photo-latent catalyst and following UV exposure, the condensation reactions will be triggered under ambient moisture conditions without the need for the aqueous environment [27]. Shang et. al. [28] synthesized a series of low hydroxyl content sols and formulated coating compositions using a photoinitiator. The coating systems were tested in terms of flame resistance in comparison with conventional samples. In another study by Chemtob et. al. [29], acidic and basic photo-catalyst generators were used for the cross-linking of silanol terminated silicone oligomers. A high percentage of cross-linking was characterized using various instrumentational techniques. Manchanda et. al. [30] also found that a photo-blocked 1, 5 diazabicyclonon-5-ene (DBN) could efficiently cure silane and acetoacetate/acrylate compounds due to generation of an in-situ superbase after UV exposure. Among different studies, some have not been able to address all of the challenges of sol-gel systems or some have not been able to achieve satisfactory properties compared to conventional wet process. In addition, there is a need to investigate UV curable sol-gel pretreatments specifically designed for corrosion protection of metallic substrates.

In this research, a UV-initiated curing mechanism (UV-sol-gel) has been used in order to obtain a polymerized network of Si-O-Si on the aluminum substrate. This technique uses UV-radiation to trigger the sol-gel process by the in-situ generation of super-acid or super-base catalysts to decrease or increase the pH of hydrolysis and condensation environment. As illustrated in **Figure 2,** the pretreatment system is composed of organosilane precursors with various backbone structures (i.e. urea and epoxy), photoacid generators (PAG) and photo-base generators (PBG), an organic solvent. The precursors were synthesized by modifying polymeric intermediates using functional alkoxysilane compounds. The cured films were characterized using Fourier transform infrared spectroscopy (FTIR), contact angle, and gravimetrical techniques.

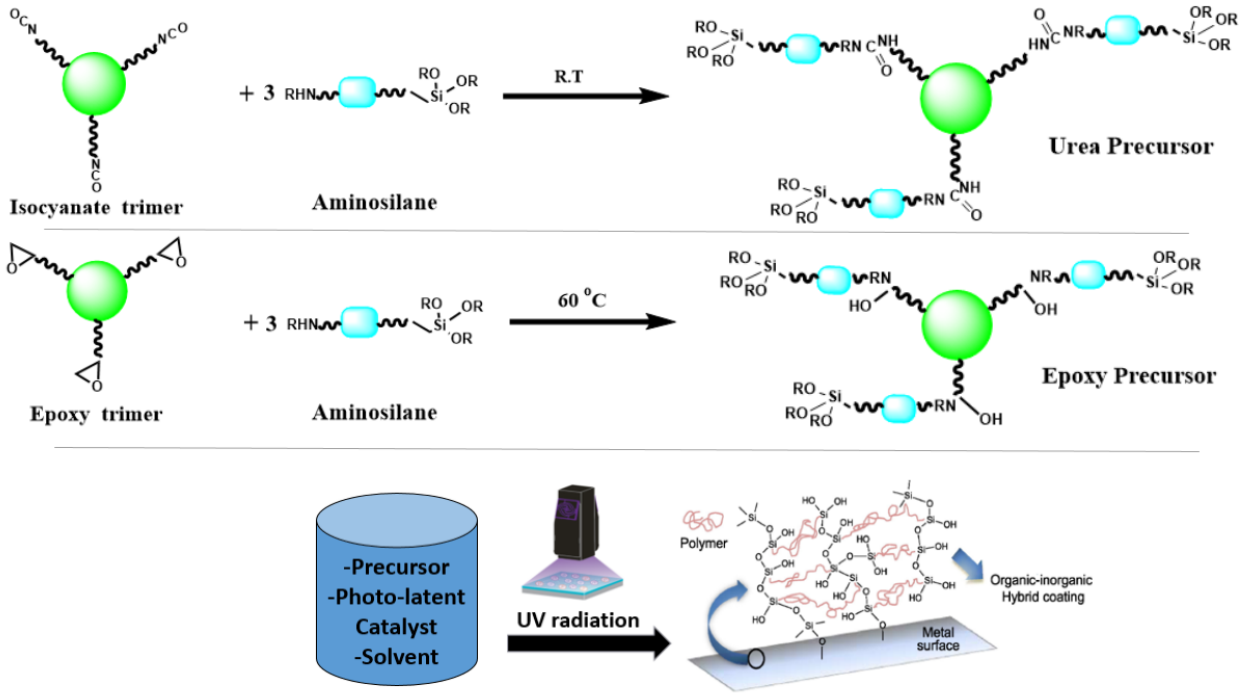

Figure 2: The chemical routes to obtain urea and epoxy precursors used in the UV-curable sol-gel pretreatment formulation

The performance of UV-sol-gel pretreatments was evaluated for corrosion resistance using quantitative techniques such as DC polarization and electrochemical impedance spectroscopy (EIS) along with the salt spray test (ASTM B117). The effects of precursor chemistry, catalyst type, and thermal post-treatment were studied in comparison with the conventional wet process. After the selection of an optimized candidate, the effect of various factors such as ambient curing time, UV energy density, and coating thickness on film performance was investigated. Finally, the possibility of using a functionalized OIH (FOIH) pretreatment with a relatively higher thickness (30 πm) in a primer-less protective coating system was studied using EIS and salt spray methods.

2. Materials and methods

2.1. materials

Aluminum alloy (Al 2024-T3) test panels with dimensions of 2” 2” were supplied by Q-panel. CGI – 90 and Irgacure 250 were used as PBG and PAG respectively, provided by BASF. 2-isopropylthioxanthone (ITX) was also used as a photo-synergist in conjunction with the photoinitiators. Ethyl alcohol, n-butanol, acetone, tetrahydrofuran (THF), acetic acid, and sodium chloride were purchased from Sigma-Aldrich. Brulin 815 GD, a proprietary detergent, was obtained from Brulin & Company Inc. Desmodur N 3390A and Joncryl 924 were also received from Covestro and BASF, respectively and used as a 2-component polyurethane topcoat. Titanium oxide (Ti-pure R670) was procured from DuPont, USA. **Figure 3** shows the chemical structure of photo-latent catalysts used in this study.

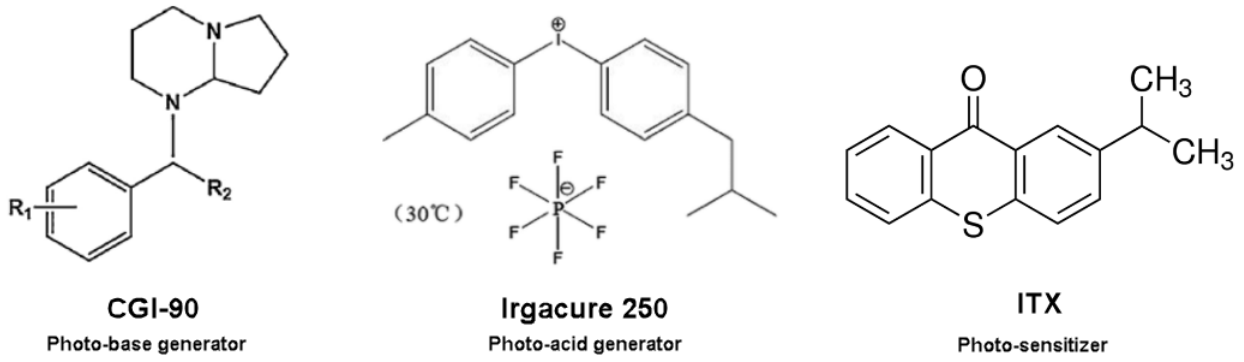

Figure 3: Chemical structure of intermediates and photo-latent catalysts used in this study

2.2 synthesis of precursors

Two different alkoxysilanes precursors containing urea or epoxy backbone with varying functionality were synthesized. Due to the ongoing intellectual property-related reasons, their detailed structure and characterization are not presented here. These precursors are hereinafter referred to as urea or epoxy precursors.

2.3 Preparation and application of pre-treatments

The aluminum alloy panels were degreased and chemically etched before the application of pretreatments as per the procedure described in an earlier study [20]. For the wet sol-gel process, considering a total of 300g of application bath, 70g of precursor solution was mixed with 127.20g of ethanol, and 81.2g of DI water. In order to adjust the pH to ~4, 22.8g of acetic acid was then added. The total precursor concentration was 20 wt.%. The mixture was stirred for 3 h before application. For UV-sol-gel process, 69g of the precursor was mixed with 231g ethanol/THF solvent and 1.8g (3 wt.% of solids) of photo-latent catalyst (PBG or PBG) together with 0.45g of ITX was added to reach the total weight of 300g at 20 wt.% of precursor concentration. All pretreatments were applied at room temperature (25–30°C) using an automatic dip coater (PTL-200, MTI Corporation), at an immersion/withdrawal speed of 17 cm/min, with a residence time of 15–20 seconds. After the application, the panels were placed vertically in a panel stacker for 15 minutes of air drying. In the case of the dry sol-gel process, panels were passed 3 times under a Fusion UV system with an H-bulb (Loctite ZETA 7415) with the conveyor belt speed set to 12 feet/min and energy density of ~0.70 J/cm^2.

In addition to varying precursor type and processing method (super-acid, super-base, and wet), some test panels were placed in an oven for 30 min to investigate the effect of thermal post-treatment. Samples were all tested after 7 days of storage at room temperature. The typical dry-film thickness obtained was ~ 7-8 microns, as measured by SEM images. For topcoats, Desmodur N 3390A (isocyanate) and Joncryl 924 (polyol) were mixed in 1:1 equivalent ratio and formulated with 10% pigment volume concentration (PVC) of TiO_2 and applied using a cubic film applicator to achieve dry film thickness of 75±5 microns. At least three replicate test panels were prepared for each test.

2.4 Characterization and test methods

FTIR spectra were collected using KBr standard disks on Bruker instrument at 64 scans and 2 cm^{-1} of resolution. The spectra obtained in the frequency range of 400-4000 cm^{-1} were used to evaluate the chemical structure of the end products. The contact angle test was carried out using an FTA-200 dynamic contact angle analyzer with a tilt-stage and environmental chamber. For gravimetrical analyses, the weight measurements were carried out using a Veritas analytical balance with an accuracy of 0.1 milligrams. A Minitab software was used for the analysis of variance among weight measurements.

The anti-corrosion properties of the specimens were studied and analyzed using DC polarization and EIS techniques through a Gamry PCI300 potentiostat connected to a three-electrode set-up (PTC1) consisting saturated calomel electrode (SCE) as a reference electrode, graphite rod as a counter electrode, and coated test specimen as a working electrode. For each sample, an area of 1 cm^2 was exposed to 3.5% NaCl solution as test electrolyte. EIS was performed in the frequency range of 0.02-10 kHz and DC polarization curves obtained at a scan rate of 1 mV/s in the applied potential range of ± 200 mV from open circuit potential. The results were analyzed using a frequency response analyzer (Echem analyst) software. The data extracted from electrochemical analysis plots represent the average of measurements on three samples. Samples were also subjected to the salt spray test conditions according to ASTM B117 up to 300h and 1000h for pretreatments and samples with pretreatment and topcoat, respectively. Then the samples were evaluated for the degree of blistering by comparison with the photographic reference standards (ASTM D714) and also the representative mean creepage of corrosion products or loss of coating extending from a scratch mark was rated based on the prescribed table (ASTM D1654).

3. Results and discussion

3.1 Characterization of curing

For both conventional (wet) sol-gel and UV-sol-gel process, the curing reaction essentially involves the conversion of alkoxysilane groups to a crosslinked siloxane network (OIH). FTIR spectroscopy was used to track the conversion of alkoxysilane groups to siloxane network. A representative FTIR spectrum, for the UV-sol-gel system containing urea precursor and CGI-90 as PBG after 7 days at room temperature is shown in **Figure 4**. A sharp and intense peak at 1087 cm^{-1} for the sample before UV-curing (related to SiOR groups) has been transformed into two distinct peaks at around 1050 cm^{-1} and 1150 cm^{-1} indicating substantial conversion of alkoxysilane groups. In fact, according to the literature, these separate peaks in the range of 1000 to 1250 cm^{-1} are generally expected to arise mostly from asymmetric stretching vibrations of Si-O-Si bridging sequences [31].

In the presence of the photo-latent PBG, which is a non-ionic photo-base generator that releases DBN upon UV exposure [30], and in-situ increase in pH triggers the formation of silanols under ambient humidity and their condensation in a relatively short time. A similar trend was also observed in the pretreatment formulation containing PAG. In that case, in-situ generation of superacid by decomposition of a diaryliodonium salt and an α-aminoketone and generation of H^+ and PF^{6-} and tertiary amine acting as efficient condensation catalysts [29]. In addition to the PAG and PBG effect, the addition of a photosensitizer (ITX) has also been reported to increase the probability of absorption in a wider range of UV [32].

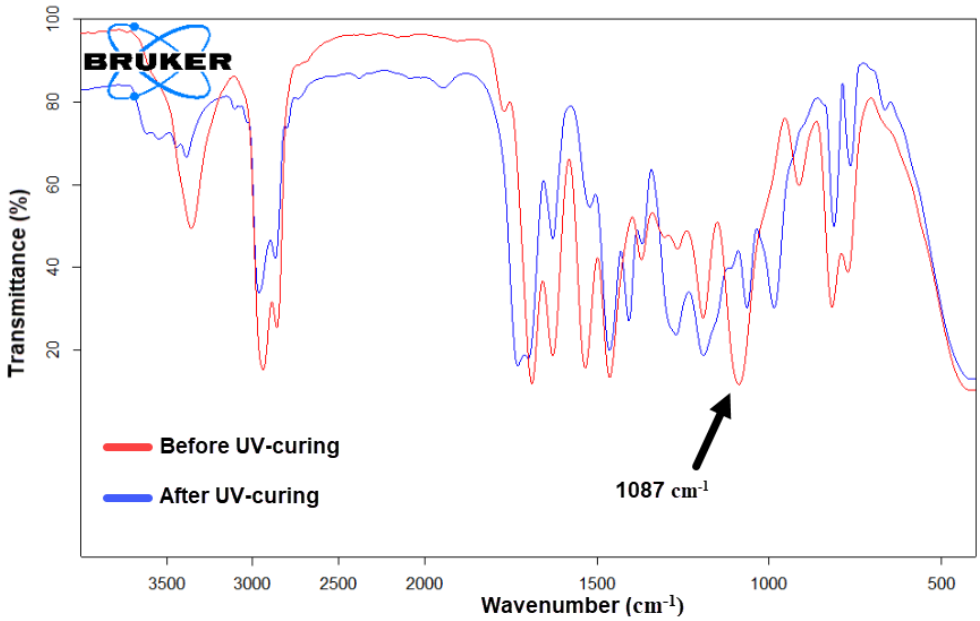

Figure 4: FTIR spectra of urea precursor before and after UV-curing

3.2. Gravimetrical analyses

One of the main objectives of this work was to investigate the difference between the curing extent and performance of pretreatments containing PAG and PBG in comparison with the conventional wet sol-gel method. Moreover, for UV-sol-gel systems, it was also thought necessary to study the effect of additional thermal post-curing on the performance of these systems, as compared to the conventional system. Therefore, a systematic study of the extent of conversion of alkoxysilane groups in UV-sol-gel pretreatments without any heat post-curing (samples designated as R) and their post-cured counterparts (samples designated as O) was carried out.

Since the cure reactions essentially involve the formation of a specific amount of alcohol and water (volatile loss) corresponding to the alkoxysilane content of the system, we used a gravimetric method for characterization of the cure extent. The initial weight of the coatings on test panels (after solvent flash-off) as well as the weight of coating after UV exposure and post-treatment (either O or R), and the coating weights after 7 days of storage were recorded using an

analytical balance (four replicates each) and the effect of catalyst system (photo-latent base or acid) and post-treatment on the observed weight loss was analyzed using statistical software. **Figure 5** represents the main effect diagrams and analysis of variance (ANOVA) results obtained from Minitab software for weight loss difference immediately after curing and post-treatment. As can be seen for **Figure 5**, the effect of catalyst type on weight loss in comparison with the wet process was not statistically significant for both types of precursors (P=0.928 and P=0.081 for urea and epoxy precursors, respectively). This suggests that the extent of curing in formulations containing photo-latent catalysts is as much as that of the conventional wet process and as seen in the main effect plots, the mean value of weight loss is even more in dry sol-gel systems. This effect was more pronounced for the epoxy precursor as the acid-catalyzed systems had greater weight loss value. The results reveal that thermal post-treatment has a significant effect on the extent of curing in all samples and this factor was found to be statistically significant, as indicated by the differences in weight loss values between the samples with and without thermal treatment (P=0.04 and P=0.05 for urea and epoxy precursors, respectively). This observation revealed that regardless of the catalyst type and curing mechanism, additional heat treatment would accelerate the curing process – which has been initiated by the release of superbase or superacid after UV exposure- leading to a higher weight loss value immediately after curing. It should also be noted that no significant interaction between the variables was observed.

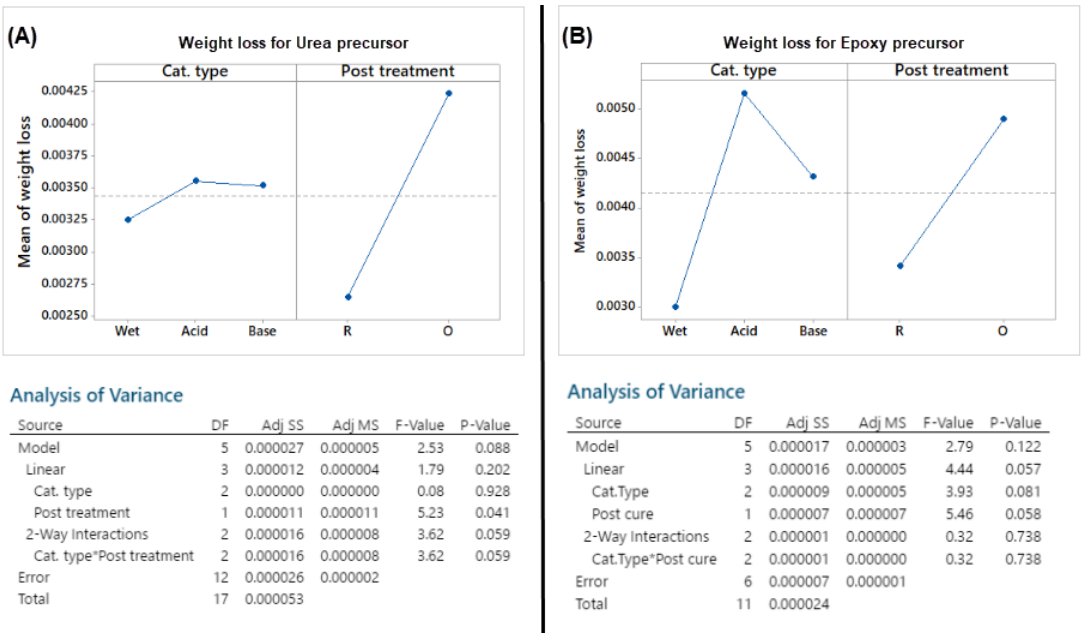

Analysis of Variance

Source	DF	Adj SS	Adj MS	F-Value	P-Value
Model	5	0.000027	0.000005	2.53	0.088
Linear	3	0.000012	0.000004	1.79	0.202
Cat. type	2	0.000000	0.000000	0.08	0.928
Post treatment	1	0.000011	0.000011	5.23	0.041
2-Way Interactions	2	0.000016	0.000008	3.62	0.059
Cat. type*Post treatment	2	0.000016	0.000008	3.62	0.059
Error	12	0.000026	0.000002		
Total	17	0.000053			

Analysis of Variance

Source	DF	Adj SS	Adj MS	F-Value	P-Value
Model	5	0.000017	0.000003	2.79	0.122
Linear	3	0.000016	0.000005	4.44	0.057
Cat.Type	2	0.000009	0.000005	3.93	0.081
Post cure	1	0.000007	0.000007	5.46	0.058
2-Way Interactions	2	0.000001	0.000000	0.32	0.738
Cat.Type*Post cure	2	0.000001	0.000000	0.32	0.738
Error	6	0.000007	0.000001		
Total	11	0.000024			

Figure 5: The gravimetrical analysis for curing of A) urea and B) Epoxy based sol-gel pretreatments immediately after curing/post-treatment P<=0.05 is considered as the significance limit

The data in figure 6 represent the weight loss values of the samples after 7-day of storage under ambient conditions, after exposure to the UV source. As can be seen, although samples with post-treatment (O samples) still had higher weight loss, the effect of post-treatment was not statistically significant anymore (P=0.325 and P=0.108) for urea and epoxy precursors, respectively) as the weight loss values had increased for R samples of UV-sol-gel systems. On the other hand, the effect of the catalyst was found to be more significant (P=0.507 and P=0.015 for urea and epoxy precursors, respectively) because of the fact that unlike wet sol-gel samples, the mean weight loss for acid and base-catalyzed UV-sol-gel sample increased substantially after 7 days at room temperature. These results suggest that in the case of UV-sol-gel samples, the condensation reaction would continue for a long time after UV exposure (dark cure) and reach the level to that of thermal post-treated samples. This can be ascribed to the presence of an active catalyst in these systems driving the condensation reaction. This observation also suggests that UV-sol-gel samples will attain performance comparable to thermal post-cured samples within 7-

days under ambient conditions, and hence do not require thermal post-treatment. This is a significant technical and environmental benefit of UV-sol-gel pretreatments.

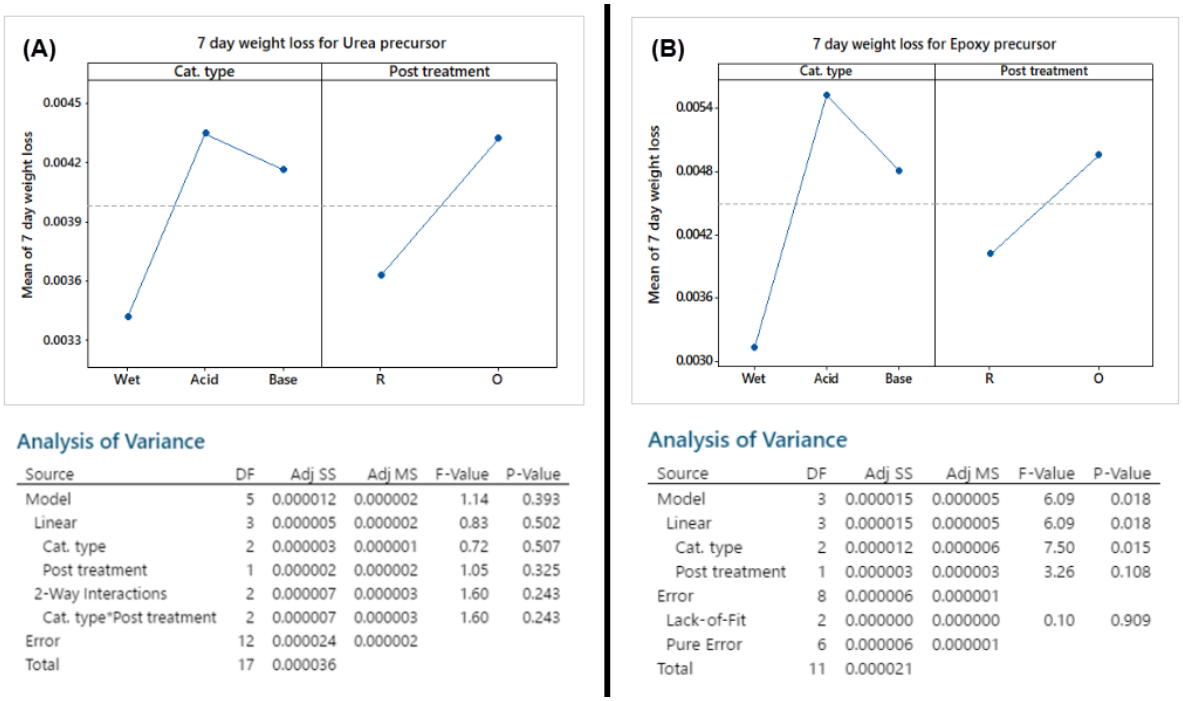

Analysis of Variance

Source	DF	Adj SS	Adj MS	F-Value	P-Value
Model	5	0.000012	0.000002	1.14	0.393
Linear	3	0.000005	0.000002	0.83	0.502
Cat. type	2	0.000003	0.000001	0.72	0.507
Post treatment	1	0.000002	0.000002	1.05	0.325
2-Way Interactions	2	0.000007	0.000003	1.60	0.243
Cat. type*Post treatment	2	0.000007	0.000003	1.60	0.243
Error	12	0.000024	0.000002		
Total	17	0.000036			

Analysis of Variance

Source	DF	Adj SS	Adj MS	F-Value	P-Value
Model	3	0.000015	0.000005	6.09	0.018
Linear	3	0.000015	0.000005	6.09	0.018
Cat. type	2	0.000012	0.000006	7.50	0.015
Post treatment	1	0.000003	0.000003	3.26	0.108
Error	8	0.000006	0.000001		
Lack-of-Fit	2	0.000000	0.000000	0.10	0.909
Pure Error	6	0.000006	0.000001		
Total	11	0.000021			

Figure 6: The gravimetrical analysis for curing of A) urea and B) Epoxy-based sol-gel pretreatments 7 days after curing/post-treatment P<=0.05 is considered as the significance limit

3.3 Contact angle measurement

One of the key effects of the sol-gel pre-treatments on various substrates is known to be to increase the surface hydrophobicity which better protection of the substrate from the corrosive environment and water penetration [33]. Contact angle measurement was carried out with the purpose of studying the effect of UV-sol-gel pretreatments on surface energy. **Table 1** summarizes the contact angle values obtained from pretreatments with different precursor type, the application process, and post-treatment combinations. The mean value of the contact angle from the three replicates was considered. Regarding the labeling, samples have been labeled in the order of "precursor type (urea or epoxy), application process (A for PAG, B for PBG, and W for the wet process), and post-treatment type (R for room temperature storage and O for thermal post-

treatment). For example, a sample with a combination of Urea-A-O represents a pretreatment system based on urea precursor that has been cured by a photo-latent photoacid generator (PAG) followed by an additional thermal post-treatment.

Table 1: The contact angle measurements for sol-gel pretreatments based on different precursors

Sample	**Urea**						**Epoxy**						**Bare metal**
	A		**B**		**W**		**A**		**B**		**W**		
	R	**O**	**R**	**O**	**R**	**O**	**R**	**O**	**R**	**O**	**R**	**O**	
Contact Angle (°)	**73.9**	**74.5**	**68.6**	**77.8**	**72.37**	**80.8**	**80.4**	**82.8**	**77.6**	**84.0**	**71.0**	**78.2**	**62.2**

Results revealed that all samples showed a significant improvement in contact angle value from that for the bare metal surface (62.2°) which indicates an effective increase in surface hydrophobicity of the pretreated panels. It was also observed that for almost all samples, the contact angle was higher for thermally post-treated samples. However, the difference in values was significantly higher for wet systems compared to UV-sol-gel pretreatment samples. This could imply the presence of more Si-O-Si linkages for UV-sol-gel pretreatments even without the thermal post-treatment. The highest contact angle value was achieved for the Urea-A-O sample with a value of 82.8°.

3.4 Anti-corrosion properties

3.4.1 Effect of precursor type, process, and post-treatment

The effect of precursor type, application and curing process, and post-treatment on anti-corrosion properties of pretreated Al substrates were studies using DC polarization, EIS and salt

spray techniques. All samples were applied at approximately 7 microns of dry film thickness. After UV exposure (and thermal post-treatment for O samples), the samples were stored at room temperature for 7 days and then were exposed to a corrosive environment. **Figures 7.a** and **7.b** represent the Tafel curves obtained from DC polarization tests for urea and epoxy precursors, respectively after 7 days of immersion in 3.5 wt.% NaCl. The quantitative data resulted from Tafel extrapolation are summarized in **Table 2.**

Results revealed that for all coating compositions, a significant reduction in corrosion current density (Icorr) was achieved in comparison with bare metal (Icorr = 298 $\mu A/cm^2$). As expected, additional thermal post-treatment had a positive effect on the corrosion resistance of pretreated samples across all the formulations. However, the difference between the performance of O and R samples was significantly less for UV-sol-gel systems compared to that of the wet process. This is consistent with the findings of contact angle measurement and suggests that for UV-sol-gel samples, a thermal post-treatment is not a critical step if there is sufficient time between the UV curing and testing. In these systems, once the superbase or superacid is generated after UV exposure, the sol-gel condensation reactions (cure reaction) would continue even in absence of UV radiation (dark cure) for a considerable time leading to very high extent of reaction. However, in the case of a conventional wet sol-gel process that extent of curing, and hence film performance is significantly dependent on hydrolysis of silanes in aqueous application bath, incomplete hydrolysis before dipping of panels in the application bath could lead to an insufficient degree of curing. Conversely, if the application is done from the bath that has passed its optimum shelf-life (partial conversion of sol to gel in the bath) poor degree of curing will result. This deficiency could only be partly compensated by thermal post-treatment to facilitate a higher extent of curing [19].

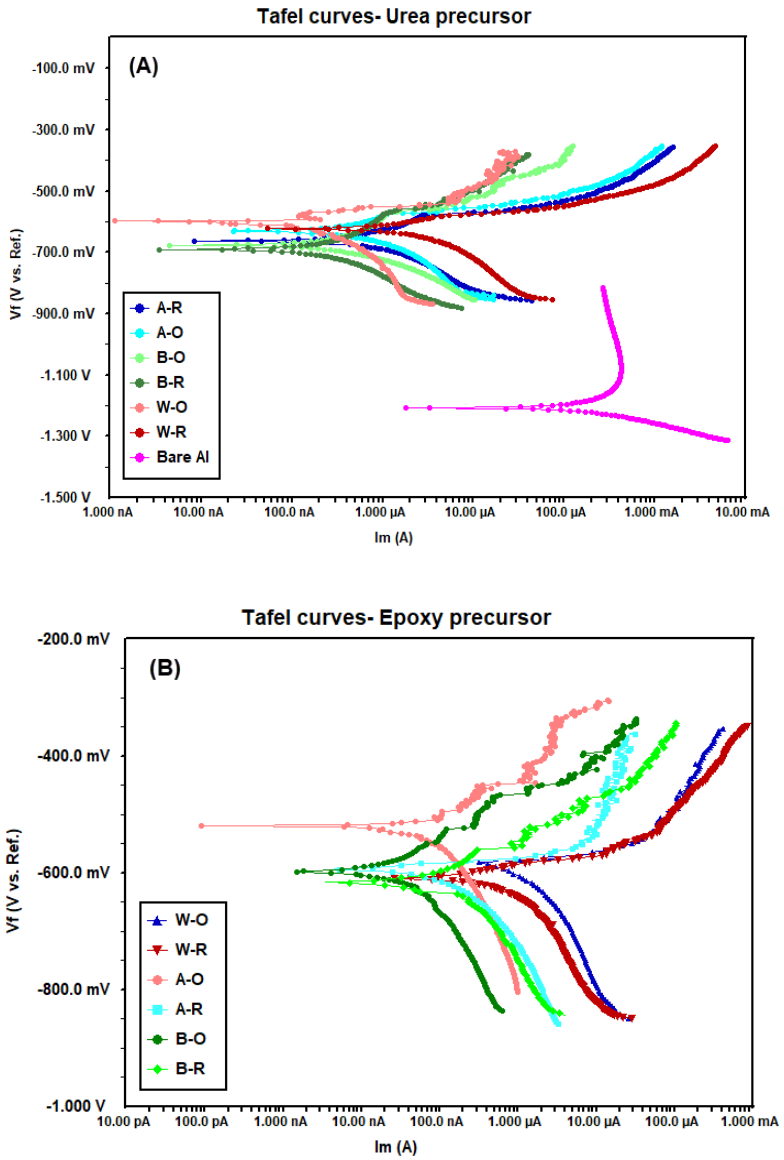

Figure 7: Tafel curves for sol-gel pretreated samples based on A)urea and B)Epoxy precursors in comparison with bare Al after 7 days of immersion in 3.5 wt.% NaCl

Table 2: DC polarization results obtained from Tafel extrapolation for sol-gel pretreated samples

Sample	Urea			Epoxy			Bare metal
	A	B	W	A	B	W	

	R	O	R	O	R	O	R	O	R	O	R	O	
Icorr ($\mu A/cm^2$)	**0.29**	**0.28**	**0.67**	**0.57**	**1.16**	**0.17**	**0.2**	**0.08**	**0.13**	**0.11**	**0.75**	**1.31**	**298**
Ecorr (mV)	**-663**	**-630**	**-691**	**-676**	**-556**	**-599**	**-594**	**-605**	**-615**	**-592**	**-608**	**-584**	**-1207**

Another important point observed from the results is the fact that corrosion current densities were significantly lower for pretreatments based on the epoxy precursor compared to the urea precursor. The I_{corr} value for the epoxy-A-O sample was as low as 0.08 $\mu A/cm^2$ while the value for the counterpart based on urea (Urea-A-O) was 0.28 $\mu A/cm^2$. This indicates the dependence of corrosion performance on the precursor chemistry. For urea samples, the wet process with post-treatment still possessed the lowest I_{corr} values while the best combination in epoxy systems (Epoxy-A-O) outperformed all other samples in the study. **Figures 8.a** and **8.b** show the bode plots obtained from EIS measurements for pretreated samples based on urea and epoxy precursors, respectively after 7 days of immersion in 3.5 wt.% NaCl solution. The impedance values at low frequencies ($|z|_{\text{ at 0.02 Hz}}$) in bode diagrams is known to be a good representative of total resistances in a coating system [34]. In addition to that, R_{pore} values which are attributed to the coating layer's resistance against corrosion media was calculated by fitting the results with an appropriate equivalent circuit [35]. The quantitative data collected from EIS tests are summarized in **Table 3**.

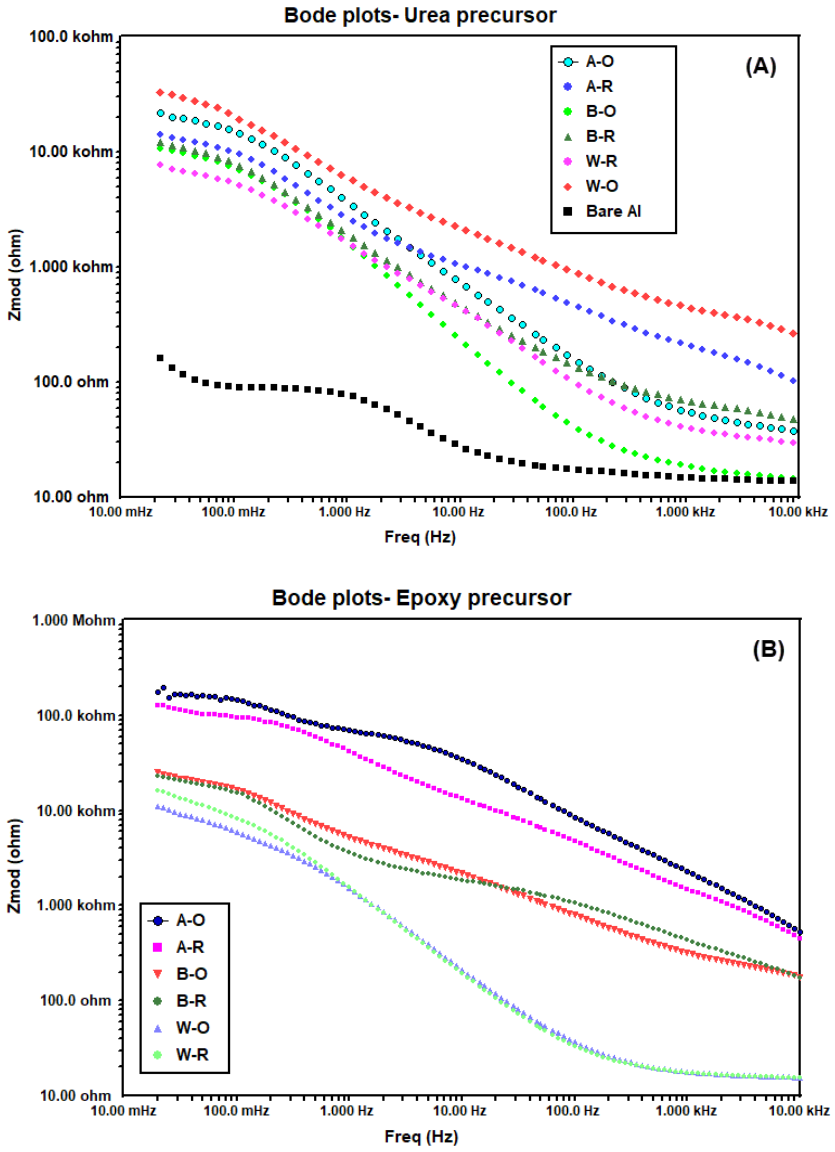

Figure 8: Bode plots for sol-gel pretreated samples based on A) urea and B) epoxy precursors in comparison with bare Al after 7 days of immersion in 3.5 wt.% NaCl

Similar trends of values were observed in EIS as the pretreated samples based on epoxy precursor showed significantly better performance compared to urea systems. The Epoxy-A-O sample had the highest impedance and R_{pore} values (175 and 148 KOhm, respectively) which outperformed the samples obtained by the conventional wet process by a large margin. Unexpected inferior properties of Epoxy-W samples could be a result of partial incompatibility of the epoxy

precursor with water as the main element of the wet process. It was also observed that PAG containing samples performed slightly better in general.

Table 3: EIS results obtained for sol-gel pretreated samples after 7 days of immersion at 3.5 wt.% NaCl

Sample	Urea						Epoxy						Bare metal
	A		B		W		A		B		W		
	R	O	R	O	R	O	R	O	R	O	R	O	
|z| at 0.02 Hz (kohm)	**14.9**	**22.8**	**11.0**	**12.3**	**7.8**	**34.6**	**127.4**	**175**	**23.0**	**24.9**	**11.1**	**16.2**	**0.11**
Rpore (kohm)	**15.8**	**24.6**	**10.3**	**12.0**	**10.4**	**31.5**	**125**	**148**	**22.3**	**26.8**	**11.9**	**15.2**	**0.09**

Table 4 shows the digital images of various samples after exposure in the salt spray chamber (ASTM B117) at different time intervals. It should be noted that only the samples with additional thermal post-treatment have been subjected to this test. The results were in complete agreement with DC polarization and EIS analyses as significantly less visual signs of corrosion and creepage of corrosion products from artificially made scribe lines were observed for epoxy samples compared to urea. Considering the results from DC polarization, EIS, and salt spray, the Epoxy-A sample was rated as the best sample formulation for further studies.

Table 4: Digital images taken from pretreated samples after different exposure times to salt spray test according to ASTM B117

Sample	Urea-A	Urea-B	Urea-W	Epoxy-A	Epoxy-B	Epoxy-W

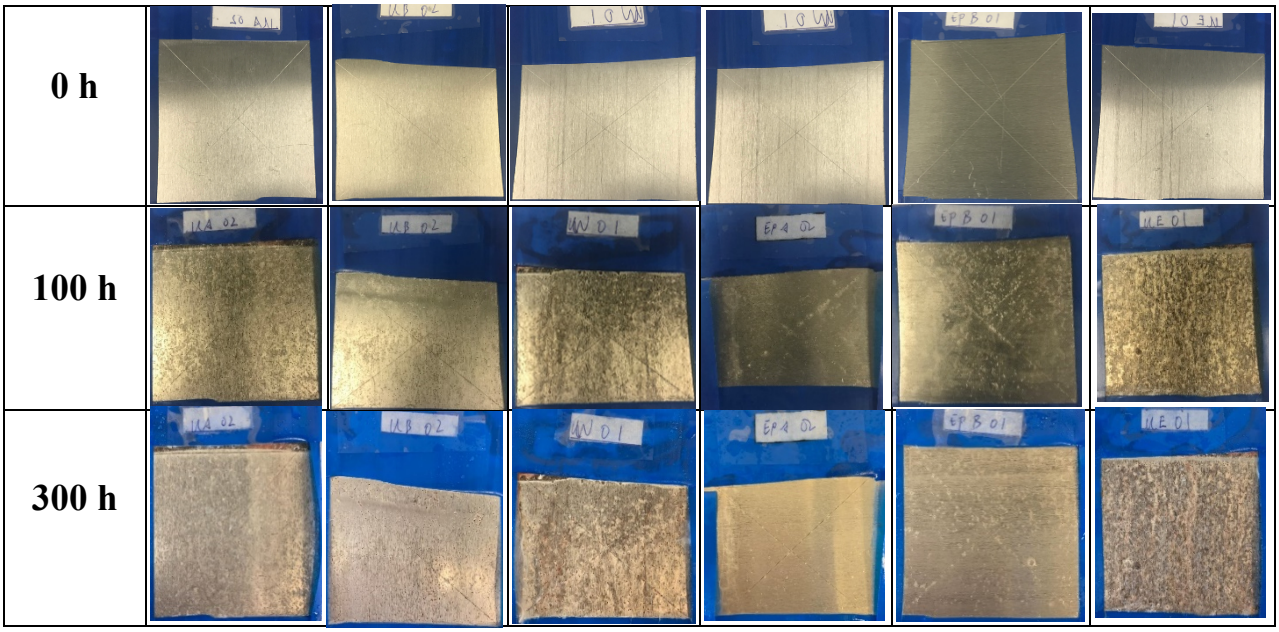

3.4.2 Effect of UV energy density

In order to investigate the effect of UV energy or dosage on the curing and performance of the pretreated samples, a representative pretreatment system sample was exposed to two significantly different levels of UV energy density. A series of samples were exposed to a total UV energy density of 2.94 j/cm^2 while the other series (high energy samples) were exposed to a total of 12.15 j/cm^2. DC polarization and EIS results were obtained and presented in **Figure 9** and **Table 5**. Results revealed that samples that were exposed to higher UV energy density performed significantly better compared to the Epoxy-A samples, with or without thermal post-treatment. The I_{corr} and $|z|_{\text{at 0.02 Hz}}$ value for Epoxy-A-R sample exposed to higher UV energy was 1.8 nA/cm^2 and 294 KOhm which was even higher than that of Epoxy-A-O sample.

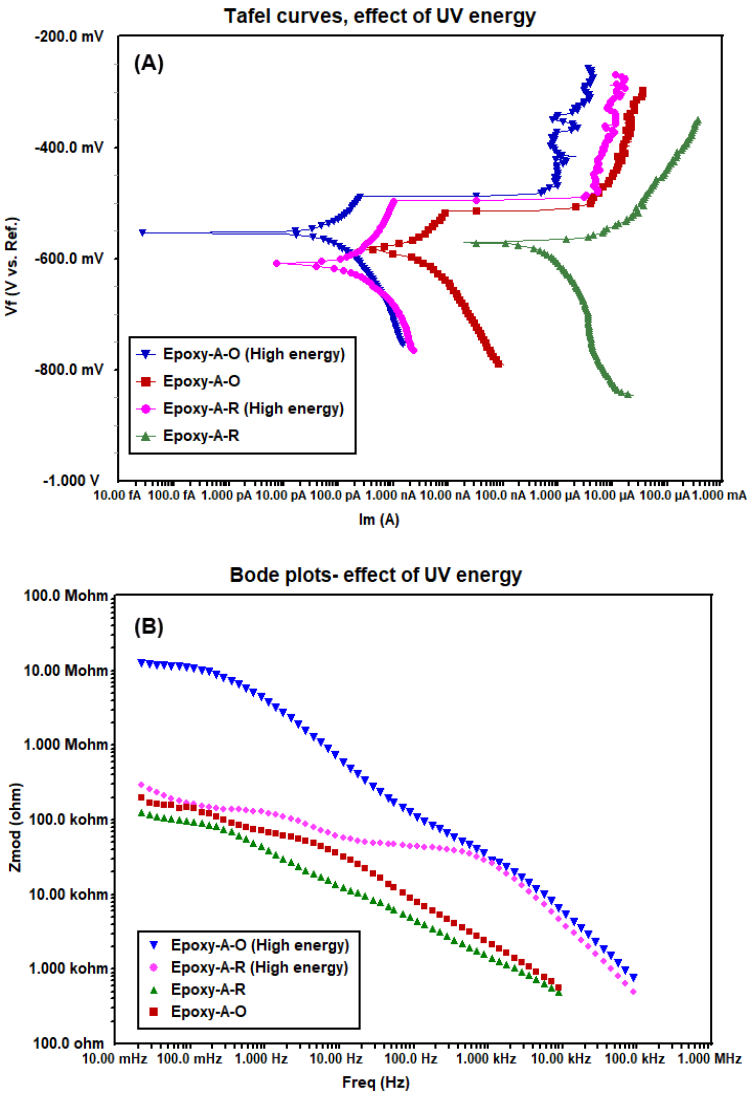

Figure 9: Effect of UV energy on A) Tafel and B) bode plots of Epoxy-A pretreatment sample on Al substrate after 7 days of immersion in 3.5 wt.% NaCl

This significant improvement in properties can be attributed either to the generation of an increased amount of acid or base catalyst or to the generation of more heat (IR component of the emission spectrum of UV lamp) accelerating the cure reaction. It is probable that both of these factors may be affecting the degree of cure. Since the lower level of UV exposure has been known to be enough to release the 3 wt.% of catalysts, the latter possibility is more likely to cause such improvement. It will be even more interesting to know that the typical I_{corr} value for a commercial Cr(VI) based pretreated Al has been found to be around 1-4 µA/cm^2 [4], [36].

Table 5: Effect of UV energy on electrochemical parameters obtained by Tafel extrapolation and EIS fitting

	Epoxy-A		Epoxy-A (High energy)	
	R	O	R	O
Icorr (μA/cm²)	0.2	0.08	0.0018	0.0012
Ecorr (mV)	-594	--605	-547	-620
|z| at 0.02 Hz (kohm)	127.4	175	12720	294
Rpore (kohm)	125	148	10872	268

3.4.3 Effect of film thickness

The effect of an increase in the thickness of the pretreatment layer was investigated by applying a three-fold thicker sample by immersion in 60 wt.% solution of Epoxy-A formulation. The resulting film thickness of the "Epoxy-A-O (high thickness)" sample was measured around 25±5 μm. As expected, EIS and salt spray results (**Figure 10** and **Table 6**) demonstrated a significant improvement in anti-corrosion properties of the OIH layer as a capacitive behavior was observed from Epoxy-A-O (high thickness) sample in bode diagram indicating that no further diffusion of corrosive elements occurred after 7 days of immersion in 3.5 wt.% NaCl solution. The images of the salt spray test (**Figure 6**) also proved the superior performance as almost no sign of blistering or growth of the corrosion products across the scratch line was observed after 300h of exposure time.

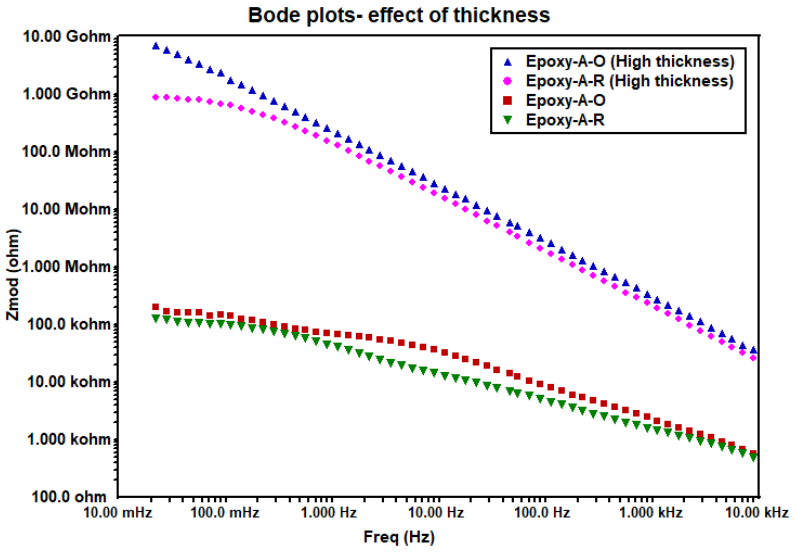

Figure 10: Effect of film thickness on electrochemical properties of Epoxy-A pretreatment on Al substrate after 7 days of immersion in 3.5 wt.% NaCl

Table 6: Effect of film thickness on salt spray results of Epoxy-A-O pretreated samples after different exposure times

Time	0h	100h	300h
Epoxy-A-O	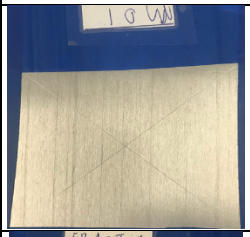	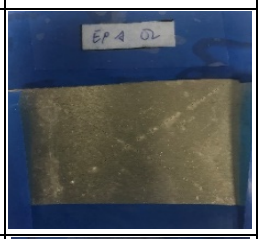	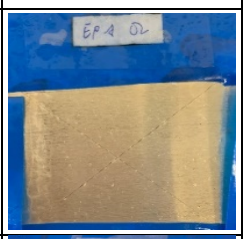
Epoxy-A-O **High thickness**	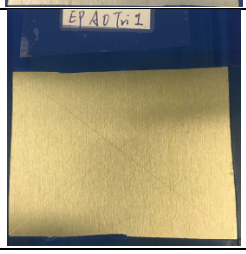	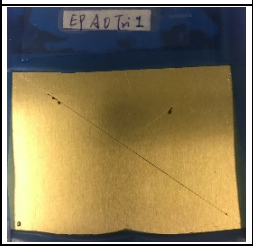	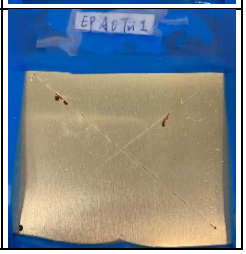

4. Conclusions

In this study, a novel UV-sol-gel process has been developed for the deposition of organic-inorganic hybrid pretreatments and its suitability and superiority over the conventional sol-gel process are demonstrated. The use of suitable photo-latent acid or photo-latent base as an initiator

for the sol-gel reaction of organo-silane precursors leads to the formation of the OIH network upon exposure to a suitable UV source under ambient humidity conditions. Both photo-latent acid and base catalysts used were found to effectively catalyze UV-sol-gel process and showed comparable cure extent. A gravimetric method was devised for cure characterization has been found to corroborate well with FTIR characterization and water contact angle measurements. A comparison of OIH pretreatments derived from the UV-sol-gel process was made with the conventional wet sol-gel process to understand the unique benefits and limitations of the UV-sol-gel process. The results revealed that the extent of curing and corrosion resistance performance of UV-sol-gel systems can be tailored by choice of alkoxysilane precursor, type of photo-latent catalyst, UV energy density and dry-film thickness. One significant finding of this study is the extent of curing and hence corrosion resistance performance of UV-sol-gel pretreatments can be improved by post-thermal treatment and using higher UV energy density. Furthermore, it has been found that UV-sol-gel pretreatments attain the very high extent of curing (comparable to that of thermal post-treated samples) within 7-days at ambient temperature, avoiding the need for expensive thermal post-treatment. Another major technical benefit of the UV-sol-gel process is the ability to prepare application baths with higher weight % of precursors which enables the development of OIH films with much higher film thickness. By harnessing these demonstrated benefits, this UV-enabled technology has many potential applications in high-performance coatingsm thin films and in advanced materials for 3D printing (additive manufacturing) applications.

5. References

[1] Y. Liu, Z. Feng, J. Walton, G. E. Thompson, P. Skeldon, and X. Zhou, “Comparison of the behaviours of chromate and sol–gel coatings on aluminium,” *Surf. Interface Anal.*, vol. 45, no. 10, pp. 1446–1451, 2013, doi: 10.1002/sia.5206.

[2] X. Zhang, C. van den Bos, W. G. Sloof, A. Hovestad, H. Terryn, and J. H. W. de Wit, “Comparison of the morphology and corrosion performance of Cr(VI)- and Cr(III)-based conversion coatings on zinc,” *Surf. Coat. Technol.*, vol. 199, no. 1, pp. 92–104, Sep. 2005, doi: 10.1016/j.surfcoat.2004.12.002.

[3] "OSHA Issues Final Standard on Hexavalent Chromium | Occupational Safety and Health Administration," 27-Feb-2006. [Online]. Available: https://www.osha.gov/news/newsreleases/national/02272006. [Accessed: 14-Jan-2020].
[4] H. Eivaz Mohammadloo, A. A. Sarabi, H. R. Asemani, and P. Ahmadi, "A comparative study of eco-friendly hybrid thin films: With and without organic coating application," *Prog. Org. Coat.*, vol. 125, pp. 432–442, Dec. 2018, doi: 10.1016/j.porgcoat.2018.09.023.
[5] V. S. Saji, "Review of rare-earth-based conversion coatings for magnesium and its alloys," *J. Mater. Res. Technol.*, vol. 8, no. 5, pp. 5012–5035, Sep. 2019, doi: 10.1016/j.jmrt.2019.08.013.
[6] H. R. Asemani, A. A. Sarabi, H. Eivaz Mohammadloo, and M. Sarayloo, "Electrochemical and morphological properties of zirconium conversion coating in the presence of nickel ions on galvanized steel," *J. Coat. Technol. Res.*, vol. 13, no. 5, pp. 883–894, Sep. 2016, doi: 10.1007/s11998-016-9800-x.
[7] Z. Feng, Y. Liu, G. E. Thompson, and P. Skeldon, "Sol–gel coatings for corrosion protection of 1050 aluminium alloy," *Electrochimica Acta*, vol. 55, no. 10, pp. 3518–3527, Apr. 2010, doi: 10.1016/j.electacta.2010.01.074.
[8] A.-P. Romano, M. Fedel, F. Deflorian, and M.-G. Olivier, "Silane sol–gel film as pretreatment for improvement of barrier properties and filiform corrosion resistance of 6016 aluminium alloy covered by cataphoretic coating," *Prog. Org. Coat.*, vol. 72, no. 4, pp. 695–702, Dec. 2011, doi: 10.1016/j.porgcoat.2011.07.012.
[9] A. Serra, X. Ramis, and X. Fernández-Francos, "Epoxy Sol-Gel Hybrid Thermosets," *Coatings*, vol. 6, no. 1, p. 8, Mar. 2016, doi: 10.3390/coatings6010008.
[10] F. Hoffmann and M. Fröba, "Vitalising porous inorganic silica networks with organic functions—PMOs and related hybrid materials," *Chem. Soc. Rev.*, vol. 40, no. 2, pp. 608–620, Jan. 2011, doi: 10.1039/C0CS00076K.
[11] R. Suleiman, H. Dafalla, and B. El Ali, "Novel hybrid epoxy silicone materials as efficient anticorrosive coatings for mild steel," *RSC Adv.*, vol. 5, no. 49, pp. 39155–39167, 2015, doi: 10.1039/C5RA04500B.
[12] L. Vivar Mora, S. Naik, S. Paul, R. Dawson, A. Neville, and R. Barker, "Influence of silica nanoparticles on corrosion resistance of sol-gel based coatings on mild steel," *Surf. Coat. Technol.*, vol. 324, pp. 368–375, Sep. 2017, doi: 10.1016/j.surfcoat.2017.05.063.
[13] K. A. Yasakau, J. Carneiro, M. L. Zheludkevich, and M. G. S. Ferreira, "Influence of sol-gel process parameters on the protection properties of sol–gel coatings applied on AA2024," *Surf. Coat. Technol.*, vol. 246, pp. 6–16, May 2014, doi: 10.1016/j.surfcoat.2014.02.038.
[14] R. Suleiman, M. Estaitie, and M. Mizanurahman, "Hybrid organosiloxane coatings containing epoxide precursors for protecting mild steel against corrosion in a saline medium," *J. Appl. Polym. Sci.*, vol. 133, no. 38, Oct. 2016, doi: 10.1002/app.43947.
[15] G. Chawada and B. Z. Dholakiya, "Organic–inorganic hybrid sol–gel pretreatments for corrosion protection of mild steel in neutral and acidic solutions," *Res. Chem. Intermed.*, vol. 41, no. 6, pp. 3659–3674, Jun. 2015, doi: 10.1007/s11164-013-1479-3.
[16] S. M. Ali and H. A. Al lehaibi, "Protective sol-gel coatings for zinc corrosion: Precursor type effect," *Surf. Coat. Technol.*, vol. 311, pp. 172–181, Feb. 2017, doi: 10.1016/j.surfcoat.2017.01.010.
[17] S. M. Ashrafi-Shahri, F. Ravari, and D. Seifzadeh, "Smart organic/inorganic sol-gel nanocomposite containing functionalized mesoporous silica for corrosion protection," *Prog. Org. Coat.*, vol. 133, pp. 44–54, Aug. 2019, doi: 10.1016/j.porgcoat.2019.04.038.

[18] D. Wang and Gordon. P. Bierwagen, “Sol–gel coatings on metals for corrosion protection,” *Prog. Org. Coat.*, vol. 64, no. 4, pp. 327–338, Mar. 2009, doi: 10.1016/j.porgcoat.2008.08.010.
[19] M. Niknahad, C. Patel, and V. Mannari, “Corrosion Protection of Aluminum Alloy by Sol-Gel Derived Organic-Inorganic Hybrid Pretreatments Based on Epoxy Resin Modified Silane Precursor,” *J. Coat. Sci. Technol.*, vol. 3, no. 1, pp. 29–40, May 2016, doi: 10.6000/2369-3355.2016.03.01.4.
[20] M. Niknahad and V. Mannari, “Corrosion protection of aluminum alloy substrate with nano-silica reinforced organic–inorganic hybrid coatings,” *J. Coat. Technol. Res.*, vol. 13, no. 6, pp. 1035–1046, Nov. 2016, doi: 10.1007/s11998-016-9814-4.
[21] V. M. Mannari, “Corrosion-resistant coatings and methods using polyureasil precursors,” US20120258319A1, 11-Oct-2012.
[22] B. Veeraraghavan, B. Haran, D. Slavkov, S. Prabhu, B. Popov, and B. Heimann, “Development of a Novel Electrochemical Method to Deposit High Corrosion Resistant Silicate Layers on Metal Substrates,” *Electrochem. Solid-State Lett.*, vol. 6, no. 2, pp. B4–B8, Feb. 2003, doi: 10.1149/1.1537092.
[23] S. Balbay, “Anti-Yellowing UV-Curable hybrid coatings prepared by the Sol–Gel method on polystyrene,” *Prog. Org. Coat.*, vol. 140, p. 105499, Mar. 2020, doi: 10.1016/j.porgcoat.2019.105499.
[24] T. Hanuhov, E. Asulin, and R. Gvishi, “Evaluation of opto-mechanical properties of UV-cured and thermally-cured sol-gel hybrids monoliths as a function of organic content and curing process,” *J. Non-Cryst. Solids*, vol. 471, pp. 301–311, Sep. 2017, doi: 10.1016/j.jnoncrysol.2017.05.043.
[25] M. Mohseni, S. Bastani, and A. Jannesari, “Influence of silane structure on curing behavior and surface properties of sol–gel based UV-curable organic–inorganic hybrid coatings,” *Prog. Org. Coat.*, vol. 77, no. 7, pp. 1191–1199, Jul. 2014, doi: 10.1016/j.porgcoat.2014.04.008.
[26] S. Senani, E. Campazzi, M. Villatte, and C. Druez, “Potentiality of UV-cured hybrid sol–gel coatings for aeronautical metallic substrate protection,” *Surf. Coat. Technol.*, vol. 227, pp. 32–37, Jul. 2013, doi: 10.1016/j.surfcoat.2013.01.051.
[27] A. Gigot, M. Sangermano, L. C. Capozzi, and K. Dietliker, “In-situ synthesis of organic–inorganic coatings via a photolatent base catalyzed Michael-addition reaction,” *Polymer*, vol. 68, pp. 195–201, Jun. 2015, doi: 10.1016/j.polymer.2015.05.019.
[28] D. Shang, X. Sun, J. Hang, L. Jin, and L. Shi, “Flame resistance, physical and mechanical properties of UV-cured hybrid coatings containing low-hydroxyl-content sols via an anhydrous sol-gel process,” *Prog. Org. Coat.*, vol. 105, pp. 267–276, Apr. 2017, doi: 10.1016/j.porgcoat.2017.01.015.
[29] A. Chemtob, H. De Paz-Simon, C. Croutxé-Barghorn, and S. Rigolet, “UV-activated silicone oligomer cross-linking through photoacid and photobase organocatalysts,” *J. Appl. Polym. Sci.*, vol. 131, no. 3, Feb. 2014, doi: 10.1002/app.39875.
[30] H. Manchanda and V. Mannari, “Super photo-base initiated organic-inorganic hybrid coatings by plural-cure mechanisms,” *Prog. Org. Coat.*, vol. 127, pp. 222–230, Feb. 2019, doi: 10.1016/j.porgcoat.2018.11.011.
[31] R. F. S. Lenza and W. L. Vasconcelos, “Structural evolution of silica sols modified with formamide,” *Mater. Res.*, vol. 4, no. 3, pp. 175–179, Jul. 2001, doi: 10.1590/S1516-14392001000300006.

[32] J. Kustra *et al.*, “Two-photon controlled sol–gel condensation for the microfabrication of silica based microstructures. The role of photoacids and photobases,” *RSC Adv.*, vol. 7, no. 74, pp. 46615–46620, Oct. 2017, doi: 10.1039/C7RA08608C.
[33] A. Hussain, J. Calabria-Holley, D. Schorr, Y. Jiang, M. Lawrence, and P. Blanchet, “Hydrophobicity of hemp shiv treated with sol-gel coatings,” *Appl. Surf. Sci.*, vol. 434, pp. 850–860, Mar. 2018, doi: 10.1016/j.apsusc.2017.10.210.
[34] H. R. Asemani, P. Ahmadi, A. A. Sarabi, and H. Eivaz Mohammadloo, “Effect of zirconium conversion coating: Adhesion and anti-corrosion properties of epoxy organic coating containing zinc aluminum polyphosphate (ZAPP) pigment on carbon mild steel,” *Prog. Org. Coat.*, vol. 94, pp. 18–27, May 2016, doi: 10.1016/j.porgcoat.2016.01.015.
[35] M. Motamedi, A. R. Tehrani-Bagha, and M. Mahdavian, “The effect of cationic surfactants in acid cleaning solutions on protective performance and adhesion strength of the subsequent polyurethane coating,” *Prog. Org. Coat.*, vol. 77, no. 3, pp. 712–718, Mar. 2014, doi: 10.1016/j.porgcoat.2013.12.009.
[36] W. Zhu, W. Li, S. Mu, N. Fu, and Z. Liao, “Comparative study on Ti/Zr/V and chromate conversion treated aluminum alloys: Anti-corrosion performance and epoxy coating adhesion properties,” *Appl. Surf. Sci.*, vol. 405, pp. 157–168, May 2017, doi: 10.1016/j.apsusc.2017.02.046.